J|A|C|S
ARTICLES
Published on Web 09/22/2004

Electrostatic Influence on Rotational Mobilities of Sol−Gel-Encapsulated Solutes by NMR and EPR Spectroscopies

Korin E. Wheeler, Nicholas S. Lees, Ryszard J. Gurbiel,‡ Shelby L. Hatch, Judith M. Nocek, and Brian M. Hoffman*

Contribution from the Department of Chemistry, Northwestern University, 2145 Sheridan Road, Evanston, Illinois 60208-3113

Received June 7, 2004; E-mail: bmh@northwestern.edu

Abstract: The rotational mobilities of small solute molecules encapsulated in tetramethyl orthosilicate (TMOS) sol−gels have been investigated by EPR spectroscopy of encapsulated nitroxide probes and by high-resolution NMR spectroscopic measurements of transferred NOE's (trNOE's), of T_1's, and of T_1's in the rotating frame ($T_1\rho$). The two spectroscopic methods are sensitive to motions on different time scales and hence, are nicely complementary. Suites of neutral, positively, and negatively charged nitroxide probes (EPR) and of simple diamagnetic small molecules (NMR) were selected to disclose influences of electrostatic interactions with the sol−gel walls and to probe the presence of multiple populations of molecules in distinct regions of the sol−gel pores. For neutral and negatively charged solute probes, both techniques disclose a *single* population with a significantly increased average rotational correlation time, which we interpret at least in part as resulting from exchange between free-volume and transiently immobilized surface populations. The electrostatic attraction between cationic probes and the negatively charged sol−gel walls causes the positively charged probes to be more effectively immobilized and/or causes a greater percentage of probes to undergo this transient immobilization. The EPR spectra directly disclose a population of cationic probes which are immobilized on the X-band EPR time scale: $\tau_c \gtrsim 10^{-7}$ s. However, NMR measurements of trNOE's and of $T_1\rho$ demonstrate that this population does exchange with the free-volume probes on the slower time scale of NMR. This approach is equally applicable to the study of solutes within other types of confined spaces, as well.

Encapsulation of organic dyes, coordination compounds, colloids, and proteins in tetramethyl orthosilicate (TMOS) derived sol−gels (SG) has been widely used for the study of reactions in confined spaces.[1−16] As a consequence, considerable attention has been devoted to understanding the motional dynamics of encapsulated solvent and solute molecules, notably through NMR measurements of solvent mobilities[17−22] and through solute luminescence depolarization studies of encapsulated probe molecules.[1,12,23−25] A picture has emerged in which SG-encapsulated molecules reside in several regions.[26] Those within the interior of a "cell" (free-liquid region) behave much as though they were in bulk solution, while those in an "interface region", at or near the walls, have more restricted motions. An additional "constraining region" is postulated to include crevices,

‡ Faculty of Biotechnology, Department of Biophysics, Jagiellonian University, Kraków, Poland.

(1) Gottfried, D. S.; Kagan, A.; Hoffman, B. M.; Friedman, J. M. *J. Phys. Chem.* **1999**, *103*, 2803−2807.
(2) Zink, J.; Valentine, J. S.; Dunn, B. *New J. Chem.* **1994**, *18*, 1109−1115.
(3) Akbarian, F.; Lin, A.; Dunn, B. S.; Valentine, J. S.; Zink, J. I. *J. Sol−Gel Sci. Technol.* **1997**, *8*, 1067−1070.
(4) Nocek, J.; Hatch, S. L.; Seifert, J. L.; Hunter, G.; Thomas, D. D.; Hoffman, B. M. *J. Am. Chem. Soc.* **2002**, *124*, 9404−9411.
(5) Pletneva, E. V.; Crnogorac, M. M.; Kostic, N. M. *J. Am. Chem. Soc.* **2002**, *124*, 14342−14354.
(6) Shibayama, N.; Saigo, S. *J. Mol. Biol.* **1995**, *251*, 203−209.
(7) Shen, C.; Kostic, N. M. *J. Am. Chem. Soc.* **1997**, *119*, 1304−1312.
(8) Ellerby, L.; Clinton, N. R.; Nishida, F.; Yamanaka, S. A.; Dunn, B.; Valentine, J. S.; Zink, J. I. *Science* **1992**, *225*, 1113−1115.
(9) Yamanaka, S. A.; Nishida, F.; Ellerby, L. M.; Dunn, B.; Valentine, J. S.; Zink, J. I. *Chem. Mater.* **1992**, *4*, 495−497.
(10) Eggers, D. K.; Valentine, J. S. *Protein Sci.* **2001**, *10*, 250−261.
(11) Das, T. K.; Khan, I.; Rousseau, D. L.; Friedman, J. M. *Biospectroscopy* **1999**, *5*, S64−S70.
(12) Castellano, F. N.; Heimer, T. A.; Tandhasetti, M. T.; Meyer, G. J. *Chem. Mater.* **1994**, *6*, 1041−1048.
(13) Maury, S.; Buisson, P.; Perrard, A.; Pierre, A. C. *J. Mol. Catal. B: Enzym.* **2004**, *29*, 133−148.
(14) McIninch, J. K.; Kantrowitz, E. R. *Biochim. Biophys. Acta-Protein Struct. Mol. Enzymol.* **2001**, *1547*, 320−328.
(15) Flora, K. K.; Brennan, J. D. *Chem. Mater.* **2001**, *13*, 4170−4179.
(16) Khan, I.; Shannon, C. F.; Dantsker, D.; Friedman, A. J.; Perez-Gonzalez-de-Apodaca, J.; Friedman, J. M. *Biochemistry* **2000**, *39*, 16099−16109.
(17) Askin, M.; Yurdakoc, K.; Gulsun, Z. *Spectrosc. Lett.* **1993**, *26*, 1039−1043.
(18) Hikichi, K. *Polym. Gels Networks* **1993**, *1*, 19−31.
(19) Spevacek, J.; Suchoparek, M. *Macromolecules* **1997**, *30*, 2178−2181.
(20) Gallegos, D. P.; Munn, K.; Smith, D. M.; Stermer, D. L. *J. Colloid Interface Sci.* **1987**, *119*, 127−140.
(21) Balcom, B. J.; Fischer, A. E.; Carpenter, T. A.; Hall, L. D. *J. Am. Chem. Soc.* **1993**, *115*, 3300−3305.
(22) Woessner, D. E.; Zimmerman, J. R. *J. Phys. Chem.* **1963**, *67*, 1590−1600.
(23) Gvishi, R.; Narang, U.; Bright, F. V.; Prasad, P. N. *Chem. Mater.* **1995**, *7*, 1703−1708.
(24) Doody, M. A.; Baker, G. A.; Pandey, S.; Bright, F. V. *Chem. Mater.* **2000**, *12*, 1142−1147.
(25) Jordan, J. D.; Dunbar, R. A.; Bright, F. V. *Anal. Chem.* **1995**, *67*, 2436−2443.
(26) Dunn, B.; Zink, J. I. *Chem. Mater.* **1997**, *9*, 2280−2291.

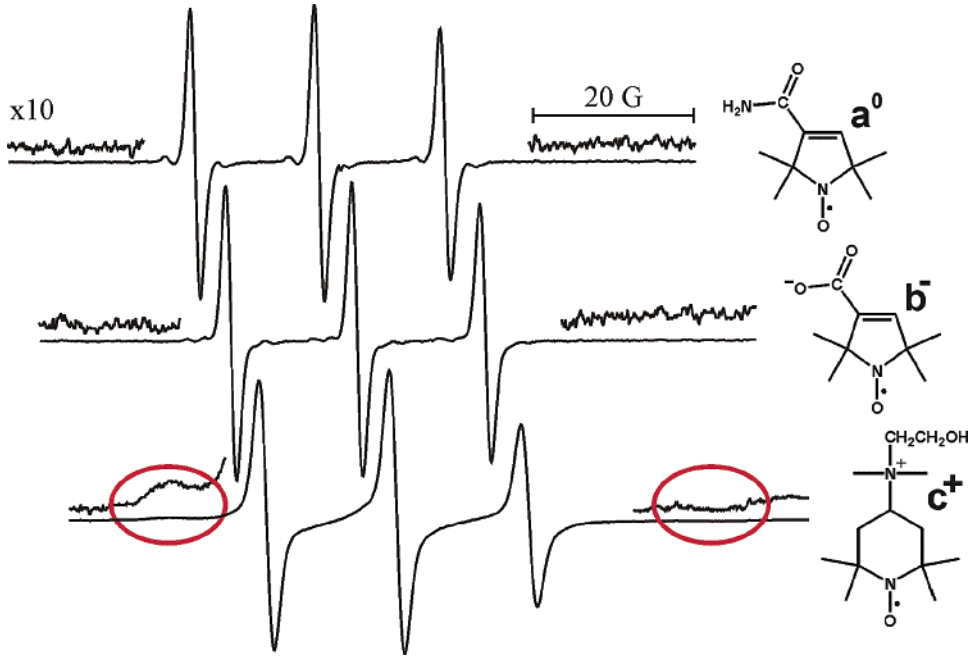

Figure 1. X-band EPR spectra of SG-encapsulated CTPY (3-carbonyl-2,2,5,5-tetramethyl-3-pyrrolin-1-yloxy (**a**^{0})), 3-Carboxy-PROXYL (3-carboxy-2,2,5,5-tetramethyl-1-pyrrolidynyloxyl, (**b**$^{-}$)), and TEMPO Choline (4-(*N*,*N*-dimethyl-*N*-(2-hydroxyethyl))ammonium-2,2,6,6-tetramethylpiperidine-1-oxyl chloride (**c**$^{+}$)). The frequency was 9.535 GHz, and the modulation amplitude was 1.0 G.

which may connect larger cells, where molecules may be more effectively immobilized.

Surprisingly, while magnetic resonance techniques have been extensively used to study the solid matrix that surrounds such confined spaces,[27] and solvents[28] or gases[29] that fill them, rarely have they been used to study the molecular motions of solutes in confined spaces. We are aware of a diffusion NMR study of the protein ubiquitin within polyacrylamide gels,[30] an HRMAS study of probe molecules interacting with chromatographic supports,[31] EPR studies of paramagnetic probes in various types of gels,[32,33] and an EPR study of spin-labeled hemoglobin within a SG.[34] We show here that EPR measurements of SG-encapsulated nitroxide spin probes and a suite of high-resolution NMR measurements of encapsulated diamagnetic probes can be combined to yield consistent information about the rotational mobilities of solute molecules, how they are influenced by electrostatic interactions between charged solutes and the negatively charged SG "cell" walls, and how solutes partition into and exchange between different regions.

Materials and Methods

Sample Preparation. All reagents were purchased from Sigma-Aldrich. Solution samples were in 10 mM potassium phosphate buffer at pH 8.0 for the EPR samples and pH 7.0 in 99.8% deuterium oxide for the NMR samples (pH are reported as read from the pH meter, with no correction for a deuterium shift). As desired, glycerol (Gly) was added to this buffer as a percentage by weight (20% for EPR and 15% for NMR samples). TMOS derived SG samples were prepared as described,[4] following the procedure of Ellerby et al.[8] The same results were obtained over a period of 48 h after gelation.

Spectroscopy. EPR spectra were collected at X-band using a modified Varian E-4 spectrometer operating at room temperature (21 °C). NMR spectra of the methylene protons of probe molecules **A**^{0} and **C**$^{+}$ and the β-carbon proton of **B**$^{-}$ were collected at 20 °C with a 600 MHz Varian INOVA600 spectrometer equipped with a 5 mm triple-resonance gradient probe. Standard pulse sequences were employed in T_1 inversion−recovery and $T_1\rho$ measurements;[35] the latter employed $\gamma B_1/2\pi = 3500$ Hz along the y axis. For trNOE measurements, two-dimensional NOESY spectra were collected and NOE peaks were integrated for mixing times of $\tau_m = 0.005$, 0.08, 0.2, 0.8, 1.0 s. The integrals were fit to

$$\mathrm{NOE}_1 = e^{-(R_1-\sigma_{IS})t_m}(1 - e^{-2\sigma_{IS}t_m}) \quad (1)$$

where $R_1 = T_1^{-1}$ (as determined by inversion recovery), to obtain the cross-relaxation rate constant, σ_{IS}, and the maximum NOE, which occurs at $\tau_m^* = \ln[(R_1 - \sigma_{IS})/(R_1 - 3\sigma_{IS})]/2\sigma_{IS}$.

Results and Discussion

EPR. Figure 1 shows the room-temperature X-band EPR spectra of a neutral nitroxide (**a**^{0}), an anion (**b**$^{-}$), and a cation

(27) Some representative citations include: (a) Brinker, C.; Scherer, G. *Sol−Gel Science: The Physics and Chemistry of Sol−Gel Processing*; Academic Press: New York, 1990. (b) Doskocilova, D.; Schneider, B.; Jakes, J. *J. Magn. Reson.* **1978**, *29*, 79−90. (c) Davis, P. J.; Deshpande, R.; Smith, D. M.; Brinker, C. J.; Assink, R. A. *J. Non-Cryst. Solids* **1994**, *167*, 295−306. (d) Pan, V. H.; Tao, T.; Zhou, J. W.; Maciel, G. E. *J. Phys. Chem. B* **1999**, *103*, 6930−6943. (e) Lindner, E.; Brugger, S.; Steinbrecher, S.; Plies, E.; Mayer, H. A. *J. Mater. Chem.* **2001**, *11*, 1393−1401. (f) Shames, A.; Lev, O.; Iosefzon-Kuyavskaya, B. *J. Non-Cryst. Solids* **1994**, *175*, 14−20. (g) Giotto, M. V.; Zhang, J. H.; Inglefield, P. T.; Wen, W. Y.; Jones, A. A. *Macromolecules* **2003**, *36*, 4397−4403. (h) Inglefield, P. T.; Jones, A. A.; Lubianez, R. P.; Ogara, J. F. *Macromolecules* **1981**, *14*, 288−292. (i) Jehng, J. Y.; Sprague, D. T.; Halperin, W. P. *Magn. Reson. Imaging* **1996**, *14*, 785−791.

(28) Additional representative citations include: (a) Hikichi, K. *Polym. Gels Networks* **1993**, *1*, 19−31. (b) Gallegos, D. P.; Munn, K.; Smith, D. M.; Sterner, D. L. *J. Colloid Interface Sci.* **1987**, *119*, 127−140. (c) Woessner, D. E.; Zimmerman, J. R. *J. Phys. Chem.* **1963**, *67*, 1590−1600.

(29) Some representative citations include: (a) Cain, E. J.; Wen, W. Y.; Jost, R. D.; Liu, X.; Dong, Z. P.; Jones, A. A.; Inglefield, P. T. *J. Phys. Chem.* **1990**, *94*, 2128−2135. (b) Simpson, J. H.; Wen, W. Y.; Jones, A. A.; Inglefield, P. T.; Bendler, J. T. *Macromolecules* **1996**, *29*, 2138−2142.

(30) Sass, H.-J.; Musco, G.; Stahl, S. J.; Wingfield, P. T.; Grzesiek, S. *J. Biomol. NMR* **2000**, *18*, 303−309.

(31) Handel, H.; Gesele, E.; Gottschall, K.; Albert, K. *Angew. Chem., Int. Ed.* **2003**, *42*, 438−442.

(32) Yalpani, M.; Hall, L. D. *Can. J. Chem.* **1984**, *62*, 975−980.

(33) Watanabe, T.; Yahagi, T.; Fujiwara, S. *J. Am. Chem. Soc.* **1980**, *102*, 5187−5191.

(34) Kar, L.; Johnson, M. E.; Bowman, M. K. *J. Magn. Reson.* **1987**, *75*, 397−413.

(35) Harris, R. K. *Nuclear Magnetic Resonance Spectroscopy*; Pitman Publishing: Marshfield, MA, 1983.

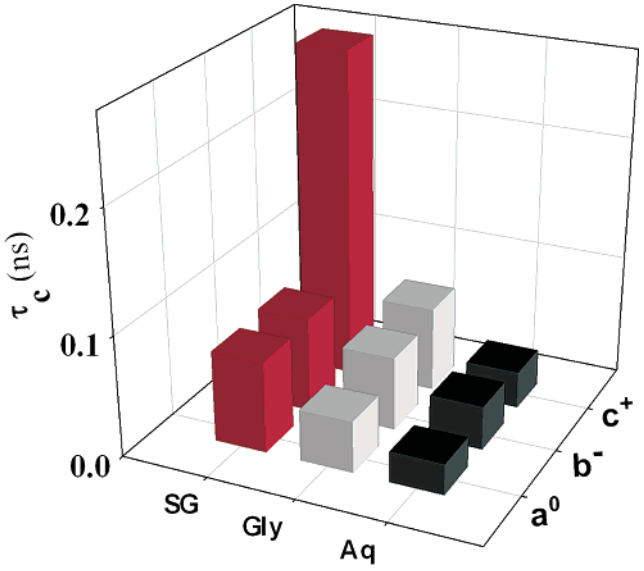

Figure 2. Rotational correlation times (τ_c) of EPR probes $\mathbf{a^0}$, $\mathbf{b}^-$, and $\mathbf{c}^+$ in sol−gel (SG), 20% glycerol (Gly), and aqueous solution (Aq).

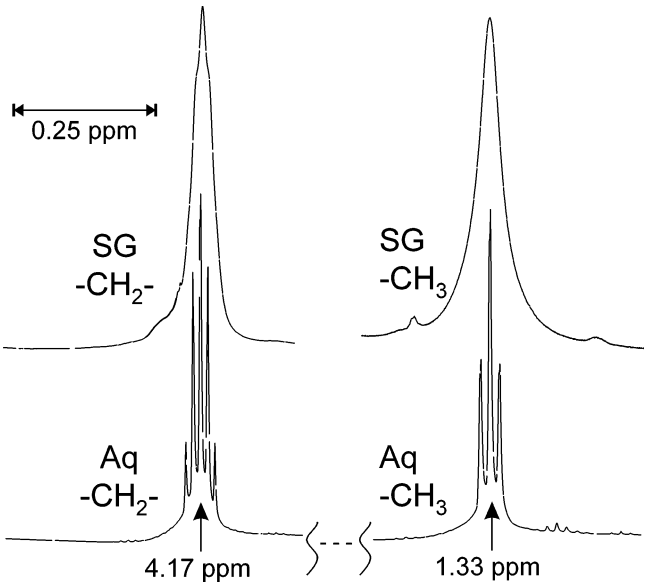

Figure 3. 1D ^{1}H NMR peaks of $\mathbf{A^0}$ in aqueous buffer and SG.

($\mathbf{c}^+$) encapsulated in SG. The three sharp lines in each spectrum are typical of a nitroxide in the motionally narrowed regime. Rotational correlation times, τ_c, have been calculated[36] from such spectra for the three nitroxides dissolved in aqueous solution, in 20% glycerol, and encapsulated in the SG (Figure 2). SG incorporation of the neutral ($\mathbf{a^0}$) and negative ($\mathbf{b}^-$) nitroxides increases τ_c modestly, by factors of ∼2. This effect is mimicked by the addition of 20% glycerol, which increases τ_c through a corresponding increase in the solution viscosity (η): $\tau_c \propto \eta$. The influence of SG encapsulation might be attributable to a corresponding increase in viscosity of solvent in the free-liquid region, but previous studies of solvent mobility[37,38] suggest that in whole or in part it reflects rapid exchange between probes with bulklike rotational mobilities that reside in the cell interior and probes at the interface that are transiently immobilized. Persistently immobilized nitroxides, $\mathbf{a^0}$ or $\mathbf{b}^-$, with τ_c and residence times of more than $\sim 10^{-6}-10^{-7}$

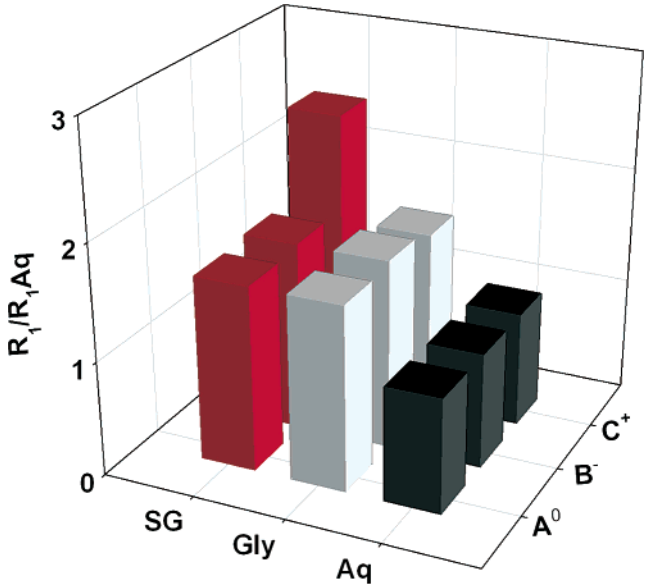

Figure 4. R_1 for $\mathbf{A^0}$, $\mathbf{B}^-$, and $\mathbf{C}^+$ in aqueous buffer, 15% glycerol buffer, and SG media.

s are not present; they would give features in the spectra at fields corresponding to the circled regions in Figure 1 (and see below), but there are no such features.

The spectra for $\mathbf{c}^+$ in the buffer and in 20% glycerol are roughly the same as for the other two nitroxides, but the spectrum of $\mathbf{c}^+$ in SG is quite different. First, SG incorporation of this positively charged probe causes a distinctly greater increase in τ_c (greater line broadening) of the mobile nitroxides (Figures 1 and 2) than seen for $\mathbf{a^0}$, $\mathbf{b}^-$, indicating that the electrostatic attraction of the cationic solute to the negative walls results in additional restrictions to motion of interface probes and/or an increase in their number.

More dramatically, the spectrum of $\mathbf{c}^+$ contains features (circled in Figure 1) corresponding to a population of spin probes that are fully immobilized within the SG. The excess broadening of the mobile spectrum of $\mathbf{c}^+$ could reflect a contribution from exchange between the mobile spins and this immobile population, but preliminary analysis suggests that this is not the case.[39]

NMR. We selected neutral triethyl phosphate ($\mathbf{A^0}$), negatively charged sodium lactate ($\mathbf{B}^-$), and positively charged triethylammonium chloride ($\mathbf{C}^+$) as a set of probe molecules with simple two-spin ^{1}H NMR patterns that exhibit an intramolecular NOE. As illustrated in the ^{1}H spectrum of $\mathbf{A^0}$ (Figure 3), the lines in the spectra of the encapsulated probe molecules are broadened such that J couplings become unresolved, which we provisionally assign to a magnetic susceptibility distribution introduced by the inhomogeneous SG. To the best of our knowledge, these are the first reported ^{1}H NMR spectra of SG-encapsulated *solute* molecules obtained with a high-resolution spectrometer.

The effective (average) τ_c values of the encapsulated NMR probes were determined through use of an inversion−recovery sequence to determine the relaxivities: $R_1 \equiv T_1^{-1} \propto \tau_c$ in the rapid-tumbling limit, $\omega_0\tau_c \ll 1$. Figure 4 presents the ratio $R_1/R_1^{aq} = \tau_c/\tau_c^{aq}$ for the three probes in aqueous solution, 15% glycerol, and SG. The 60% increase in R_1 for $\mathbf{A^0}$ and $\mathbf{B}^-$ upon

(36) Miller, W. G. In *Spin Labeling II. Theory and Applications*; Berliner, L. J., Ed.; Academic Press: New York, 1979; pp 173−221.

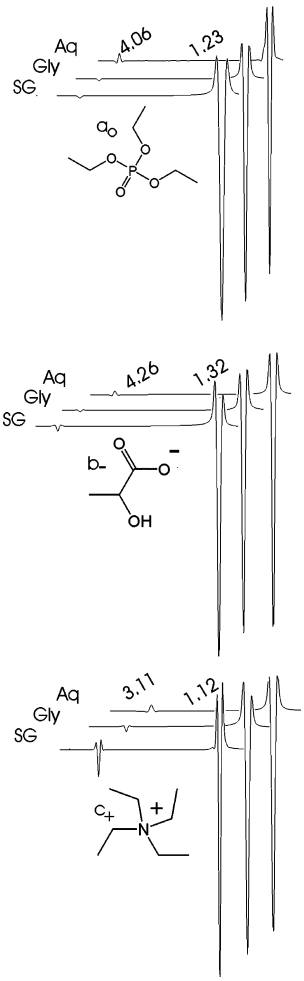

Figure 5. 1D slices of 2D NOESY spectra of aqueous, glycerol/buffer, and SG samples for NMR probes $\mathbf{A^0}$, $\mathbf{B}^-$, and $\mathbf{C}^+$ (τ_m = 100 ms). Slices were chosen at the maximum enhancement of the saturated peak. The chemical shifts in ppm are indicated for the saturated peak, the methyl peak, and the trNOE cross-peak.

their encapsulation in the SG is matched by the increased viscosity of the glycerol solution. As with the EPR probes, R_1 for the mobile cationic $\mathbf{C}^+$ probe shows a much greater increase in the SG than it does for the $\mathbf{A^0}$ and $\mathbf{B}^-$ probes.

We have tested for exchange between mobile and constrained probe populations by measurements of transferred NOEs (trNOEs) and of T_1 in the rotating frame ($T_1\rho$). A trNOE enhancement is observed in the NMR spectrum of rapidly tumbling molecules in confined spaces when they exchange with a slowly tumbling population.[31] For a two-spin homonuclear system in the fast-tumbling limit ($\tau_c \rightarrow 0$), the NOE is $+1/2$; in the slow-motion limit, the NOE is -1. Small molecules tumbling in solution typically fall in the "crossover" regime, exhibiting small, positive NOE's,[31,40] and this is so for all three probes in aqueous buffer (Figure 5). The small increase in viscosity when $\mathbf{A^0}$ and $\mathbf{B}^-$ are dissolved in 15% glycerol (increases in τ_c) only changes their NOE's from slightly positive to slightly negative. The NOE peak of $\mathbf{C}^+$ in the SG does *not* correspond to that seen in 15% glycerol/buffer: instead, it is large and negative (Figures 5 and 6). We assign this change to the NOE transferred to the mobile $\mathbf{C}^+$ in the pore interior through exchange with a population of $\mathbf{C}^+$ with restricted motion, namely in the interface or constraining regions of the SG.

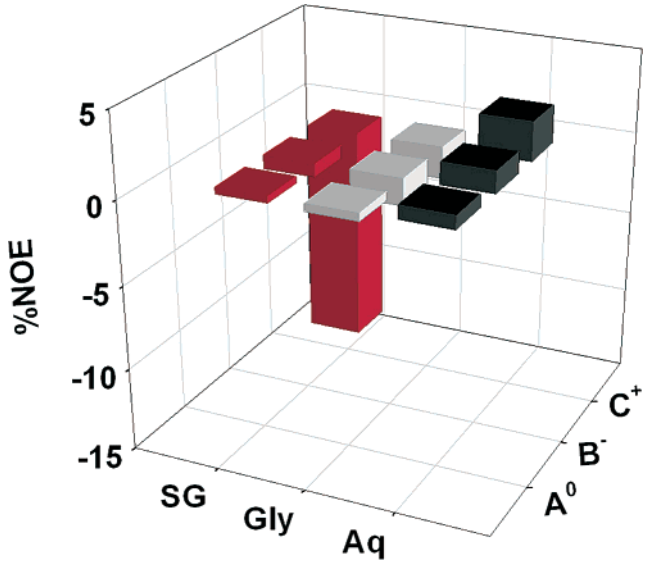

Figure 6. Percent NOE enhancement of the methyl peak of each of the NMR probes $\mathbf{A^0}$, $\mathbf{B}^-$, and $\mathbf{C}^+$ in aqueous, 15% glycerol/buffer, and SG media. The percent NOE was taken at τ_m = 100 ms, where NOE enhancement is at a maximum for all samples.

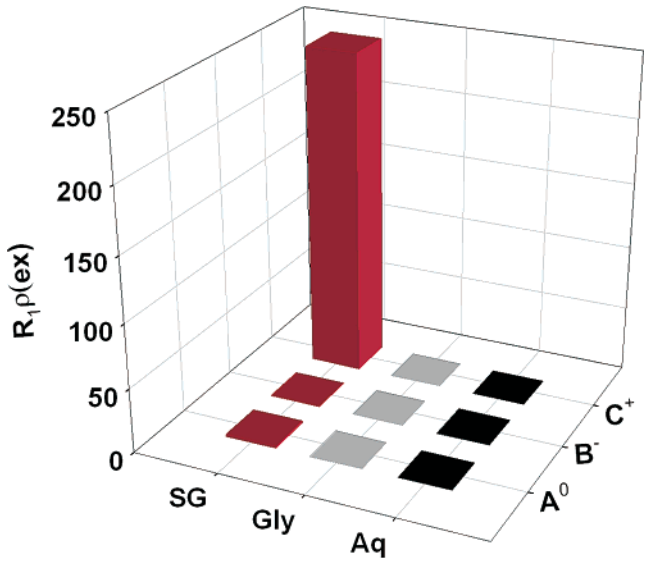

Figure 7. $R_{1\rho}$(ex) for NMR probes $\mathbf{A^0}$, $\mathbf{B}^-$, and $\mathbf{C}^+$ in aqueous, 15% glycerol/buffer solution, and SG.

The trNOE occurs in the "relaxation limit" of exchange between populations,[41] $\omega_{ex} \gg R_1$, and as a result it is not possible to analyze the trNOE for information about the size of the populations or the rate of exchange between fluid and immobile probes.[40] However, $T_1\rho$ is sensitive to exchange between mobile probes in the cell interiors and those constrained at the interface.[35,37,38] T_1 is influenced by random motions with spectral densities in the vicinity of $\omega_o \approx \gamma B_0 \approx 10^9$ s^{-1} at 600 MHz, whereas $T_1\rho$ is affected by motions with spectral densities in the vicinity of $\omega_1 \approx \gamma B_1 \approx 10^4$ s^{-1} for the present experiments. Hence, motions and/or chemical exchange with frequency $\sim\omega_1$ will alter $T_1\rho$ without affecting T_1, as reflected in the difference $R_{1\rho}(\text{ex}) \equiv T_1\rho^{-1} - R_1$. Figure 7 presents $R_{1\rho}$(ex) for the three NMR probes in each medium. For the aqueous and 15% glycerol/buffer solutions, $R_{1\rho}(\text{ex}) \approx 0$ for all three probes, as expected. For $\mathbf{A^0}$ and $\mathbf{B}^-$ in SG, $R_{1\rho}(\text{ex}) \approx 0$ as well, confirming the idea that these probes sample a single, average fluid

environment that is subject to small effects from exchange between pore interior and surface. However, for $\mathbf{C}^+$ in the SG, $R_{1\rho}(\mathrm{ex}) \approx 10^2$, dramatically demonstrating an enhanced importance of exchange (at $\sim\omega_1$) between mobile $\mathbf{C}^+$ in the bulklike solution of the cell and $\mathbf{C}^+$ that is in the interface/constraining regions and whose motion is more efficiently restricted by electrostatic attraction to the SG walls.

Conclusions

EPR and high-resolution NMR techniques have disclosed that neutral and negatively charged solute probes encapsulated in an SG behave as a *single* average population on the time scales of both NMR and EPR measurements. However, the average rotational correlation times of the probes are significantly greater than those in bulk aqueous buffer, and we interpreted this as resulting from exchange between free-volume probes and a transiently immobilized, surface population.

The EPR spectra further disclose that the electrostatic attraction of a positive probe with the walls does generate a population of immobilized probes that do not exchange with the mobile ones on the time scales set by these at X-band EPR measurements, $\tau_c \gtrsim 10^{-7}$ s. Direct observation of such immobilized positive probes is not possible in a high-resolution ^{1}H NMR spectrometer, but we propose that the striking effects seen in trNOE and $T_1\rho$ measurements on the cationic probes originate in exchange between this immobile population and the mobile probes on the slower NMR time scale.

Thus, the EPR and NMR measurements not only are fully self-consistent but also, with their differing time scales, are nicely complementary. We suggest that future studies of processes in the confined spaces provided by TMOS SGs, and indeed processes of all other systems that generate confined spaces, can profitably employ either approach, depending on the goals of the study, with the advantages of their joint application available as needed.

Acknowledgment. We gratefully acknowledge NIH support of this research (Grant GM58890; HL13531). We thank Prof. J. B. Lambert for insightful discussions on NMR methodology, Dr. Benjamin Ramirez for his technical assistance with NMR, and Prof. Bruce Robinson for sharing his expertise on spin-label dynamics.

JA046659C

(37) Liu, G.; Li, Y.; Jonas, J. *J. Chem. Phys.* **1991**, *95*, 6892−6901.
(38) Wonorahardjo, S.; Ball, G.; Hook, J.; Moran, G. *Magn. Reson. Imaging* **1998**, *16*, 511−513.
(39) Robinson, B. H., personal communication.
(40) Clore, G. M.; Gronenborn, A. M. *J. Magn. Reson.* **1982**, *48*, 402−417.
(41) Neuhaus, D.; Williamson, M. P. *The Nuclear Overhauser Effect in Structural and Conformational Analysis*; VCH: New York, 1989.